

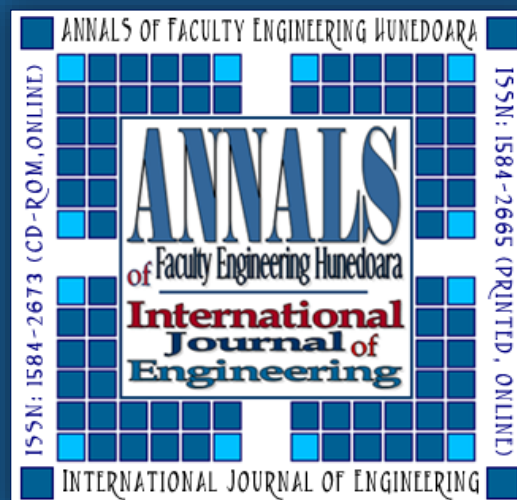
# ANNALS of Faculty Engineering Hunedoara – International Journal of Engineering

Tome XIV [2016] – Fascicule 1 [February]

ISSN: 1584-2665 [print; online]

ISSN: 1584-2673 [CD-Rom; online]

a free-access multidisciplinary publication  
of the Faculty of Engineering Hunedoara



1. Traian MAZILU

## ON THE STRUCTURAL VIBRATION OF THE RAILWAY WHEEL

<sup>1</sup>. University Politehnica of Bucharest, Department of Railway Vehicles, Bucharest, ROMANIA

**ABSTRACT:** Wheel-rail vibration has many important practical consequences, including the rolling noise, the wear of the rolling surfaces and the mechanical resistance of the vehicle and track structures. Level of the vibration of the wheel-rail system depends mainly on the vibration characteristics of both wheel and rail. In this paper, the axial and radial vibration of the wheel is studied using both theoretical and experimental approaches. Models of the wheel vibration are based on the continuous elastic body theory, respectively the vibration theory of a ring. The influences of the tread characteristics on the radial natural frequencies are pointed out. Also, the radial and axial receptances of the wheel are determined from the theoretical and experimental view point.

**Keywords:** wheel, radial vibration, axial vibration, eigenmode

### 1. INTRODUCTION

When one wheel charged under static load is running on a rail, both rail and wheel vibrate. Wheel-rail vibration is essentially a structural vibration with a frequency range that spans a very wide range it starts from around 20 Hz and may reach up to 5 kHz. Wheel-rail vibration has two main sources of excitation. On the one hand, it is about of the parametric excitation due to the variability of the track stiffness, especially in the vertical plane, which is related by the sleepers, and on the other hand, it is about of the irregularities of the rolling surfaces, including the discontinuities of the rails (joints, crossings, switches) [1, 2].

Consequences of the wheel-rail vibration are multiple and serious. In this connection, it can identify a few areas of practical interest in which the studies regarding the wheel-rail vibration can be applied, namely, mechanical resistance of the vehicle structure and the track, the wear of the surfaces rolling [3] and noise pollution [4].

Wheel-rail vibration wheel-rail can be regarded as being in a system composed of three distinct subsystems: the wheel, the rail and the wheel-rail contact, and studied separately.

As regards wheel vibrations, which we treat them in this work, they are divided in two categories, radial vibration and axial vibration. Shape of the wheels with rigid assembling them in the axle of the wheel set with dynamic forces of the wheel-rail contact are decisive for the types of their modes of vibration on which wheels they are developing. Thus, the vertical and longitudinal dynamic forces are source of the radial vibration excitation, and the lateral dynamic forces generate the axial vibrations of the wheel.

The regime of radial vibrations of the wheel exhibits some particular aspects depending on frequency range which are interested in. These aspects are determined by itself wheel configuration, inertial and elastic characteristics of the different parts of them, as well as by the fact that the wheel is rigidly mounted on axle. Of the three parts of the wheel - hub, the disc and the wheel tread, the firmest is the hub which in addition is also jointly and severally liable with the axle. In the case of radial vibrations, the tread has the inertia greater than that of the disc which is more elastic.

At low and mid frequencies, the radial vibrations of the wheel are influenced by the bending vibration of the axle. In this frequency range, the hub and the wheel tread vibrate practically as a single mass. In this way, the wheel vibrates as an unsprung mass attached to axle. At higher frequencies, the wheel tread vibration tends to be decoupled from the vibration of the hub due to disc elasticity. In this situation, wheel vibrations are dominated by those of the tread. With respect to axial vibrations of the wheel, they are dominated by vibrations of tread which has the axial stiffness much less than radial one.

In this work, models for the study of the radial and axial vibrations of the wheel are presented. These models are based on continuous elastic body theory, which may be a fair representation of the distribution of the inertia mass. In the last section of the work, the wheel characteristics are determined experimentally on the basis of wheel response to an impulse.

**2. MODEL FOR RADIAL VIBRATION OF THE WHEEL**

As shown, in the high frequency range, wheel vibrations are dominated by the tread vibration which can be studied using the model from Figure 1 [5]. The wheel tread is considered to be a ring with average radius  $r$  with mass per length unit  $m_c$  and mass moment of the cross section  $I_r$  in respect to the neutral axle of the radial bending. The wheel web is modelled using elastic elements uniform distributed on the inside of the tread; the radial stiffness is  $k_r$  and the tangential stiffness is  $k_t$ .

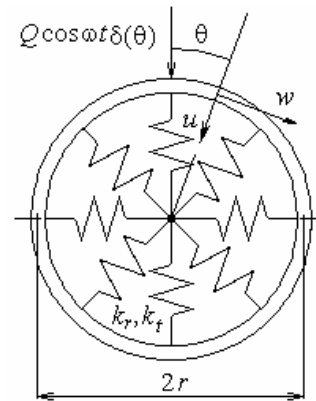


Figure 1. Wheel tread model

The harmonic force  $Q \cos \omega t$  acts on the tread, where  $Q$  is the amplitude,  $\omega$  - the angular frequency and  $t$  stands for the time. The analytical expression of the harmonic force is one of the distributed force, according to the relation  $q(\theta, t) = (Q/r) \cos \omega t \delta(\theta)$ .

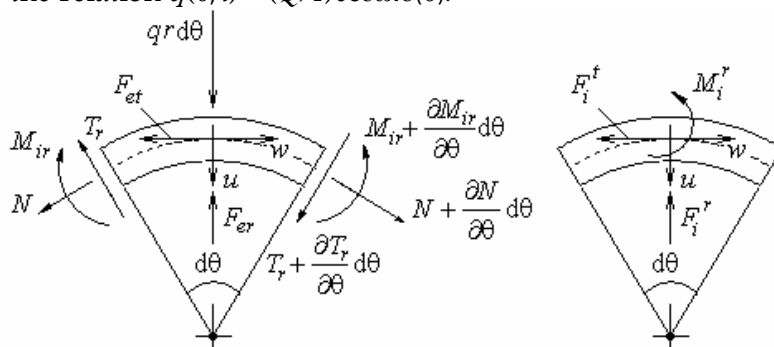


Figure 2. Radial loading of infinitesimal element of the tread.

Writing the equations of motion, it considers an infinitesimal element of tread and the forces and moments which act on this element (Figure 2): the distributed force  $q$ , normal force  $N$ , shear force  $T_r$ , bending moment  $M_{ir}$ , radial and tangential inertia forces  $F_i^r$  and  $F_i^t$ , inertia moment  $M_i^r$  and elastic forces  $F_{er}$  and  $F_{et}$

$$F_i^r = m_c r \frac{\partial^2 u}{\partial t^2} d\theta, \quad F_i^t = m_c r \frac{\partial^2 w}{\partial t^2} d\theta, \quad M_i^r = \rho I_r r \frac{\partial^2 \varphi}{\partial t^2} d\theta, \tag{1}$$

$$F_{er} = k_r u r d\theta, \quad F_{et} = k_t w r d\theta, \tag{2}$$

where the stiffnesses  $k_{r,t}$  are calculated with the relation [5]

$$k_r = k_t = \frac{n d E}{2r}, \tag{3}$$

where  $d$  is the average thickness of the wheel disc,  $E$  - Young's modulus and  $n$  corresponds to the vibration eigenmode of the tread.

Applying D'Alembert's principle, the equation of radial motion is

$$\frac{\partial T_r}{\partial \theta} + N - k_r u r - m_c r \frac{\partial^2 u}{\partial t^2} + q r = 0 \tag{4}$$

and the equation of tangentially motion is

$$-T_r + \frac{\partial N}{\partial \theta} - k_t w r - m_c r \frac{\partial^2 w}{\partial t^2} = 0. \tag{5}$$

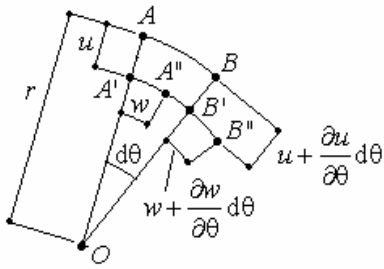


Figure 3. Radial deformations of the tread element.

Also, it writes the equation of the bending moments

$$-T_r r + \frac{\partial M_{ir}}{\partial \theta} - \rho I_r r \frac{\partial^2 \varphi}{\partial t^2} = 0. \quad (6)$$

Equations of motion of the wheel tread have to be completed with the relations between displacements. Figure 3 shows the deformations of the neutral fibre of the tread element.

The length of AB arch is  $r d\theta$ , and its deformation is given by relation

$$\Delta l = A'B' - AB = (r - u)d\theta - w + w + \frac{\partial w}{\partial \theta} d\theta - r d\theta = \left( \frac{\partial w}{\partial \theta} - u \right) d\theta. \quad (7)$$

Deformation of the arch AB is the effect of the normal force and because of that

$$\frac{\Delta l}{r d\theta} = \frac{N}{ES} \quad (8)$$

and then, inserting (7) in (8),

$$\frac{\partial w}{\partial \theta} - u = \frac{rN}{ES}. \quad (9)$$

Rotation angle of the cross sections of the tread element can be calculated with the relation

$$\varphi = \frac{\partial u}{r \partial \theta} + \frac{w}{r} - \frac{T_r}{\kappa GS}, \quad (10)$$

where  $\frac{\partial u}{r \partial \theta}$  is the contribution of the radial displacement of the neutral fibre,  $w/r$  – the angle due to the tangential displacement of the cross section and  $-T_r/(\kappa GS)$  is the contribution of the shear force with  $\kappa$  – the shear constant.

On the other hand, the rotation angle of the cross section depends on the bending moment

$$\frac{\partial \varphi}{\partial \theta} = -\frac{M_{ir}}{EI_r}. \quad (11)$$

Equations (4-6) and (9-11) describe the motion of the wheel tread. Neglecting the inertial effect of the cross sections rotation and the effect of the shear force on the rotation angle, it obtains

$$\frac{EI_r}{r^4} \left( \frac{\partial^6 u}{\partial \theta^6} + 2 \frac{\partial^4 u}{\partial \theta^4} + \frac{\partial^2 u}{\partial \theta^2} \right) + k_r \frac{\partial^2 u}{\partial \theta^2} - k_t u + m_c \left( \frac{\partial^4 u}{\partial \theta^2 \partial t^2} - \frac{\partial^2 u}{\partial t^2} \right) = \frac{\partial^2 q}{\partial \theta^2}. \quad (12)$$

Natural frequencies of the wheel tread are

$$\omega_n = \frac{1}{r^2} \sqrt{\frac{EI_r n^2 (n^2 - 1)^2 + (k_t + n^2 k_r) r^4}{m_c (n^2 + 1)}}. \quad (13)$$

Figure 4 shows the first four eigenmodes of the wheel tread.

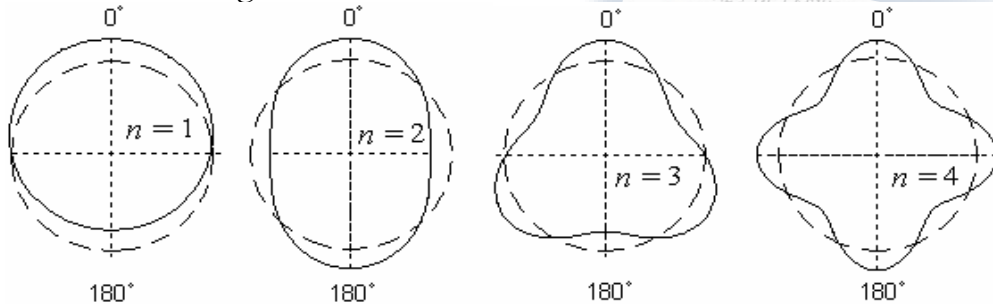


Figure 4. Eigenmodes of the wheel tread (n = 1 to 4).

Next, the influence of some parameters on the natural frequencies of the wheel tread is analysed. It considers the following values for the wheel tread parameters:  $m_c = 79.5 \text{ kg/m}$ ,  $d = 20 \text{ mm}$  and  $I_r = 4,75 \cdot 10^{-6} \text{ m}^4$ . Figure 5 shows that the natural frequencies of the radial eigenmodes increase when the wheel diameter decreases. This aspect has to be related to the low-pass filter effect due to the contact patch. When the wheel diameter becomes smaller, the natural frequency of particular eigenmode could be higher than the cut-on frequency of the low-pass filter due to the contact patch. In this way, the rolling noise could be smaller.

In time, the tread parameters change their values due to the wear. Figure 6 shows that the natural frequencies of the eigenmodes of the tread increase when the tread thickness is smaller due to the wear. This fact has similar effect mentioned above and the rolling noise could be smaller.

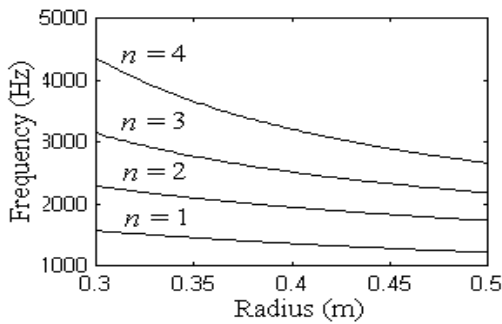


Figure 5. Wheel radius influence on the natural frequencies of the tread (radial vibration).

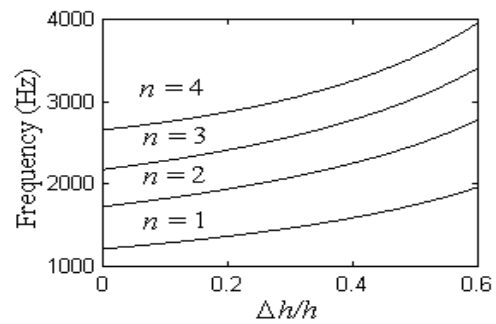


Figure 6. Tread thickness influence on the natural frequencies of the tread (radial vibration).

Although the natural frequencies can be computed with the help of the model relations with relatively good accuracy, the response in the low frequency range remains problematic. This is due to the fact that the tread vibration is coupled with the axle vibration via wheel hub.

Next, to calculate the tread response, it is necessary to consider the influence of the wheel hub (Figure 7). Basically, this involves changing first eigenmode of vibration.

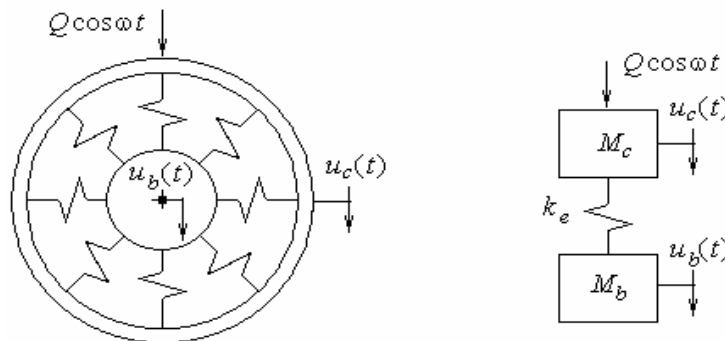


Figure 7. Equivalent model to simulate the influence of the wheel hub.

Hub and tread are connected by elastic elements distributed and they move only vertical. Hub mass ( $M_b$ ) contains 1/3 of axle mass, and the tread mass is given by the relation

$$M_c = \int dm_c = \int_0^{2\pi} r m_c d\theta = 2\pi r m_c . \tag{14}$$

Equivalent model consists of two rigid bodies for the hub and wheel tread connected by an equivalent elastic element. The equivalent stiffness has the expression

$$k_e = \pi r (k_r + k_t) , \tag{15}$$

where  $k_r$  is radial stiffness and  $k_t$  – tangential stiffness.

Equations of motion take the shape:

$$M_c \ddot{u}_c + k_e (u_c - u_b) = Q , \quad M_b \ddot{u}_b + k_e (u_b - u_c) = 0 , \tag{16}$$

where  $u_c$  is the tread displacement (as rigid body) and  $u_b$  is the hub displacement.

Considering the steady-state harmonic behaviour, the tread receptance can be calculated with the first eigenmode of vibration modified. Using the following notations

$$\mu = \frac{M_c}{M_b} , \quad \omega_1 = \sqrt{\frac{k_e (M_c + M_b)}{M_c M_b}} ,$$

the tread receptance is given by the relation

$$\bar{\alpha}_r(\theta) = \frac{1}{\omega^2 (M_c + M_b)} + \frac{1}{M_c (1 + \mu) (\omega_1^2 - \omega^2 + j\eta_1 \omega_1^2)} + \sum_{n=2}^{\infty} \frac{\cos n\theta}{M_n (\omega_n^2 - \omega^2 + j\eta_n \omega_n^2)} , \tag{17}$$

where  $\eta_n$  is the structural damping of the  $n$  eigenmode.

Figure 8 shows the radial receptance of the wheel considering the parameters values as above, in a frequency range between 100 Hz and 5 kHz. The wheel receptance from the model without the

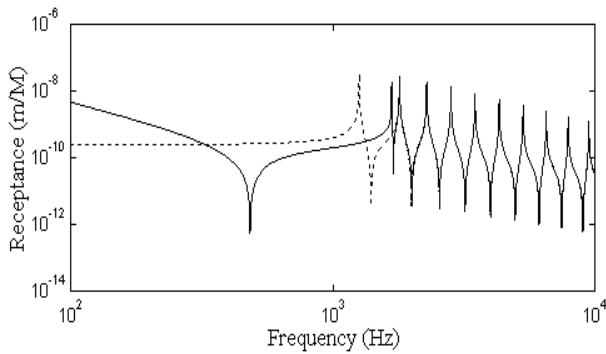


**Figure 8.** Radial receptance of the wheel: ..... only tread; — tread with hub.

hub is also represented. In this case, the receptance is constant up to 1 kHz due to the stiffness of the wheel disc. First resonance has the frequency of 1261 Hz. Then, at higher frequencies, the tread response is dominated by the alternation of resonance and antiresonance frequencies.

The tread receptance up to 1000 Hz is atypical compared with the experimental results. They show that the wheel has essentially inertial behaviour and not elastic. In fact, the wheel receptance decreases with increasing the frequency, and only after the threshold of 1500 Hz, the tread exhibits resonance frequencies.

The natural frequency of the tread coupled with the hub is 1678 Hz, value very close to the frequency of the second eigenmode of the tread (1798 Hz). It can be seen that the influence of the hub-tread coupling is significant up to the second eigenmode frequency, then this influence disappears.

### 3. AXIAL VIBRATION OF THE WHEEL

Wheel axial vibration behaviour can be studied with the model of the ring with axial bending and torsion. [5, 7]. Figure 9 shows the outline of the wheel tread model which is considered as a free ring without elastic connection with the wheel disc. This has an axial stiffness negligible compared to that of the tread, which is why his influence can be ignored.

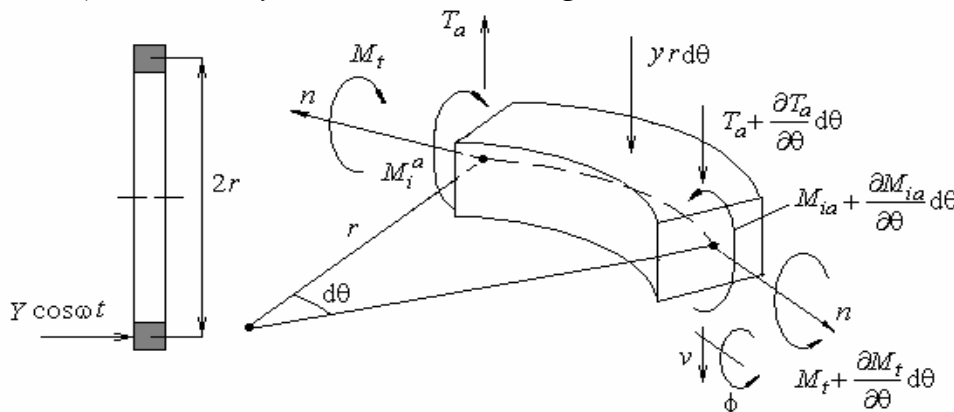


**Figure 9.** Axial loading of infinitesimal element of the tread.

It is considered that a lateral force  $Y \cos \omega t$  acts in the neutral axis of the tread, where  $Y$  is the force amplitude and  $\omega$  is the angular frequency. This force corresponds to the dynamic component of the guiding force.

Shear forces  $T_a$  and  $T_a + \frac{\partial T_a}{\partial \theta} d\theta$ , axial bending moments  $M_{ia}$  and  $M_{ia} + \frac{\partial M_{ia}}{\partial \theta} d\theta$ , and torsion moments  $M_t$  and  $M_t + \frac{\partial M_t}{\partial \theta} d\theta$  act on the cross sections of the tread (see Figure 9). Also, the lateral distributed force acts on the tread element

$$y = \frac{Y}{r} \cos \omega t \delta(\theta). \quad (18)$$

The tread element has the lateral displacement  $v$ , rotation angle of the cross section axle  $\alpha$  and angle of twist  $\phi$

Inertia force and moments have the following relations

$$F_i^a = m_c r \frac{\partial^2 v}{\partial t^2} d\theta, \quad M_i^a = \rho I_a r \frac{\partial^2 \alpha}{\partial t^2} d\theta, \quad M_i^t = J r \frac{\partial^2 \phi}{\partial t^2} d\theta, \quad (19)$$

where  $I_a$  is the inertia moment of the tread cross section, and  $J$  is the mass moment of inertia per length unit ( $J = \rho I_p$  with  $I_p$  – the polar moment of inertia of the cross section and  $\rho$  – the density);

$M_a^i$  is the moment of inertia due to the cross sections rotation, and  $M_t^i$  is the moment of inertia due to the torsion.

Considering the small angle  $d\theta$ , the equations of motion are as follows:

» for axial motion

$$\frac{\partial T_a}{\partial \theta} + yr - m_c r \frac{\partial^2 v}{\partial t^2} = 0. \tag{20}$$

» for torsion

$$\frac{\partial M_t}{\partial \theta} - M_{ia} - Jr \frac{\partial^2 \phi}{\partial t^2} = 0 \tag{21}$$

» for axial bending

$$T_a r - \frac{\partial M_{ia}}{\partial \theta} - M_t - \rho I_a r \frac{\partial^2 \alpha}{\partial t^2} = 0. \tag{22}$$

Also, it has to consider the following equations:

» for rotation of the cross section axle (due to the lateral displacement  $v$  and the shear force  $T_a$ )

$$\alpha = \frac{v + \frac{\partial v}{\partial \theta} d\theta - v}{rd\theta} - \frac{T_a}{\kappa GS} = \frac{\partial v}{r\partial \theta} - \frac{T_a}{\kappa GS}. \tag{23}$$

» for the torque

$$M_t = C_t \psi, \tag{24}$$

where  $\psi$  is the specific angle of torsion and  $C_t = GS^4 / (40I_p)$  is the torsional rigidity and  $S$  - the cross section area.

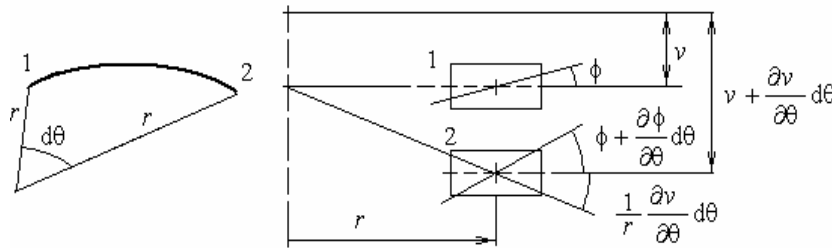


Figure 10. Explaining the specific torsion.

Specific torsion is given by the relation (see Figure 10)

$$\psi = \frac{\phi + \frac{\partial \phi}{\partial \theta} d\theta - \phi}{rd\theta} + \frac{1}{r} \cdot \frac{\partial v}{\partial \theta} = \frac{1}{r} \frac{\partial \phi}{\partial \theta} + \frac{1}{r^2} \frac{\partial v}{\partial \theta}. \tag{25}$$

Relation between the bending axial moment and the infinitesimal element curvature is

$$\frac{\partial^2 v}{r^2 \partial \theta^2} - \frac{\phi}{r} = -\frac{M_{ia}}{EI_a}, \tag{26}$$

where the first term of the curvature is given by the axial displacement and the second one, by the torsion.

Equations (20-22) and (23-26) describe the axial vibration of the wheel tread.

Neglecting the influence of the shear force and considering for the torque and the bending moment the following relations

$$M_t = \frac{C_t}{r} \left( \frac{\partial \phi}{\partial \theta} + \frac{1}{r} \frac{\partial v}{\partial \theta} \right), M_{ia} = \frac{EI_a}{r} \left( \phi - \frac{\partial^2 v}{r \partial \theta^2} \right), \tag{27}$$

the equations of motion result as:

$$\frac{EI_a + C_t}{r^2} \frac{\partial^2 v}{\partial \theta^2} + \frac{C_t}{r} \frac{\partial^2 \phi}{\partial \theta^2} - \frac{EI_a}{r} \phi - Jr \frac{\partial^2 \phi}{\partial t^2} = 0, \tag{28}$$

$$\frac{EI_a}{r^2} \frac{\partial^4 v}{\partial \theta^4} - \frac{C_t}{r^2} \frac{\partial^2 v}{\partial \theta^2} + m_c r^2 \frac{\partial^2 v}{\partial t^2} - \rho I_a \frac{\partial^4 v}{\partial t^2 \partial \theta^2} - \frac{EI_a + C_t}{r} \frac{\partial^2 \phi}{\partial \theta^2} = yr^2. \tag{29}$$

Axial receptance of the wheel tread can be calculated as follows

$$\bar{\alpha}_a(\theta) = -\frac{1}{M_c \omega^2} + \frac{1}{\pi} \sum_{n=1}^{\infty} \frac{1}{\Delta_n} (J\omega^2 r^2 - n^2 C_t - EI_a) \cos n\theta. \quad (30)$$

Figure 11 shows the axial receptance of the wheel tread calculated against the loaded point ( $\theta = 0$ ). It can be seen that the general allure is characterised by the alternation between the peaks of resonance and the deeps of antiresonance.

**4. EXPERIMENTAL DETERMINATION OF THE DYNAMIC RESPONSE OF THE WHEEL**

This section presents the experimental results on the frequency response of the wheel obtained on basis of a radial impulse excitation applied to the tread of the wheel. In this way, the radial response of the wheel and also the axial response are exhibited. Former response appears because the fact that the running surface of the wheel is conic and due to that the radial impulse excitation has an axial component. On the other hand, the wheel is not symmetric and the axial eigenmodes and the radial eigenmodes are more or less coupled. Experimental results from the acceleration spectra reveal both resonance and antiresonance frequencies [8].

The system used to determine the dynamic response of the wheel includes two accelerometers and the system data acquisition and processing. Two piezoelectric accelerometers Brüel & Kjær of type 4514 are used for acceleration measurement. One of the accelerometers is mounted on the rolling surface of the wheel tread for radial acceleration measurement and the other on the lateral face of the tread for axial acceleration (see Figure 12). Natural frequency of the accelerometers is 20 kHz and allows accurate measurements in the frequency range of interest, respectively up to 3000 Hz.

Equipment of acquisition and processing experimental data is the assembly of chassis of acquisition and data-processing NI cDAQ-9174 type and NI 9234 serial module for data stream reception and synthesis of the two accelerometers. The measurement system is connected to a laptop which is implemented in LabVIEW software.

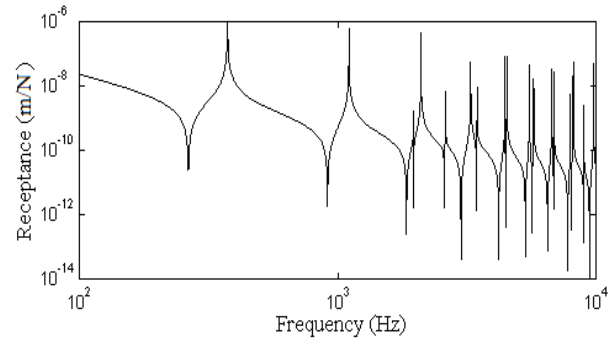


Figure 11. Axial receptance of the wheel tread.



Figure 12. Accelerometers on the rolling surface and lateral surface of the wheel tread.

Equipment of acquisition and processing experimental data is the assembly of chassis of acquisition and data-processing NI cDAQ-9174 type and NI 9234 serial module for data stream reception and synthesis of the two accelerometers. The measurement system is connected to a laptop which is implemented in LabVIEW software.

Equipment of acquisition and processing experimental data is the assembly of chassis of acquisition and data-processing NI cDAQ-9174 type and NI 9234 serial module for data stream reception and synthesis of the two accelerometers. The measurement system is connected to a laptop which is implemented in LabVIEW software.

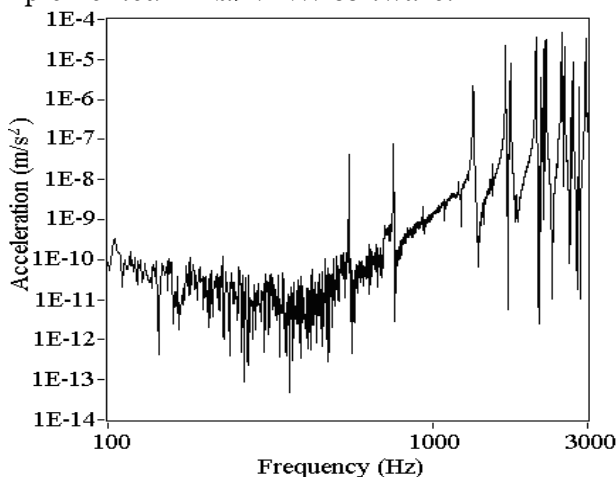


Figure 13. Radial frequency response of the wheel.

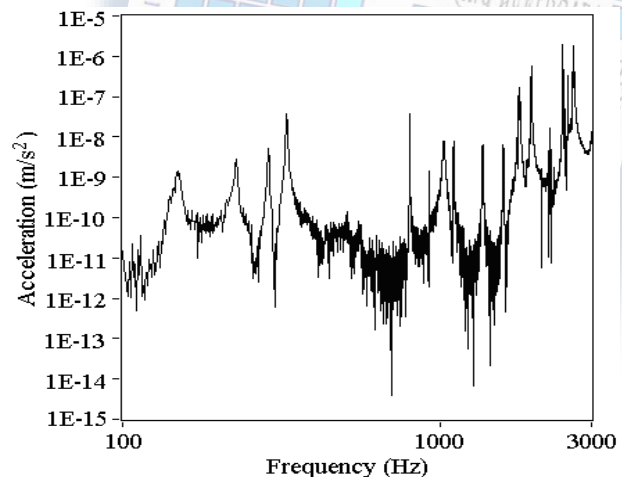


Figure 14. Axial frequency response of the wheel.

Figure 13 depicts the frequency response of the wheel in the radial direction, and Figure 14 shows the frequency response of the wheel in the axial direction. It is noted that the radial wheel frequencies are located at frequencies higher than 1500 Hz. On the other hand, at low and middle frequencies, the acceleration spectrum decreases due to the influence of the bending axle. Regarding the axial frequency response, this is richer in resonances in the middle frequency range due to the elasticity of the wheel disc.

#### **5. COMMENTS AND CONCLUSIONS**

Due to its asymmetric design, the wheel exhibits both radial and axial structural vibrations which are coupled. The radial vibrations have the natural frequencies located after 1500 Hz. Basically, at this frequency the vibrations of the tread and hub tend to be decoupled.

Axial vibrations have their natural frequencies lower due to the elasticity of the wheel disc, which is higher in the axial direction.

Radial vibrations of the wheel are excited by the overlapping of the rolling surfaces roughness and they generate the rolling noise. Axial vibrations of the wheel occur when the vehicle negotiates small curve due to the stick-slip phenomenon and they generate the squeal noise. All this kind of noises is influenced by the structural vibration of the wheel.

#### **References**

- [1.] Mazilu, T., Wheel rail vibrations (in Romanian), Ed. MatrixRom, Bucharest, 2008.
- [2.] Sebeşan I., Mazilu, T., Vibrations of the railway vehicles (in Romanian), Ed. MatrixRom, Bucharest, 2010
- [3.] K.H. Oostermeijer, „Review on short pitch rail corrugation studies”, in *Wear*, 265, 2008, pp. 1231–1237.
- [4.] D.J. Thompson, C.J.C. Jones, „A review of the modelling of wheel/rail noise generation”, in *Journal of Sound and Vibration*, 231, 2000, pp. 519–536.
- [5.] Remington, P. J., Wheel/rail rolling noise, I: Theoretical analysis, *Journal of Acoustical Society of America*, Vol. 81, no. 6, 1987.
- [6.] Mazilu, T., Comfort at rolling stock (in Romanian), Ed. MatrixRom, Bucharest, 2003.
- [7.] Grassie, S. L., Gregory, R. W., Johnson, K. L., The behaviour of railway wheelsets and track at high frequencies of excitation, *Journal Mechanical Engineering Science*, vol. 24, (1982), pag. 103-111.
- [8.] Mazilu, T., Dumitriu, M., Vibration of railway vehicles. Experimental applications, (in Romanian), Ed. MatrixRom Publishing, Bucharest, 2013.



ANNALS of Faculty Engineering Hunedoara  
– International Journal of Engineering



copyright © UNIVERSITY POLITEHNICA TIMISOARA,  
FACULTY OF ENGINEERING HUNEDOARA,  
5, REVOLUTIEI, 331128, HUNEDOARA, ROMANIA  
<http://annals.fih.upt.ro>